Recent advances on ion cyclotron resonance heating scenarios for Divertor Tokamak Test facility

Claudia Salvia[1,*], *Alessandro* Cardinali[2], *Carmine* Castaldo[3], *Silvio* Ceccuzzi[3,4], *Dirk* Van Eester[5], and *Fabio* Zanon[6]

[1]University of Padova, Centro Ricerche Fusione, Corso Stati Uniti 4, Padova, 35127, PD, Italy
[2]INFN-LNS, Via S. Sofia 62, Catania, 95125, CT, Italy
[3]ENEA, Nuclear Dept., Via Enrico Fermi 45, Frascati, 00044, RM, Italy
[4]DTT S.c.a.r.l., Via Enrico Fermi 45, Frascati, 00044, RM, Italy
[5]Laboratory for Plasma Physics, ERM/KMS, Av. de la Renaissance 30, Brussels, 1000, Belgium
[6]Eni SpA, Via delle Industrie 39, Marghera, 30175, VE, Italy

Abstract. An analysis of Ion Cyclotron Resonance Heating propagation and single-pass absorption in Divertor Tokamak Test facility (DTT) heating scenarios has been performed using the 1D full-wave code TOMCAT. This study aimed to explore a broader parameter space compared to previous works, with the goal of improving the understanding of DTT heating performance. Heating schemes at 3T and 6T were analyzed, simulating different plasma compositions with varying concentrations of D, ^{3}He, and H, across a frequency range from 50 to 90 MHz. A very promising reduced-field configuration is presented. Furthermore, three-ion heating schemes for the full-field configuration were investigated, leading to the identification of an efficient scenario. Additional analyses with TORIC and EVE were carried out, providing positive validation of the results obtained with TOMCAT.

1 Introduction

The study of plasma production and heating in the ion cyclotron range of frequencies (ICRF) has a long history in fusion research. A primary objective of this line of investigation is to optimize scenarios for effective auxiliary heating using ICRF techniques. Investigations of ICRF plasma heating have been carried out in pure hydrogen, deuterium, and helium gases, in the minor regime and in mixture of these gases.

DTT [1] —a superconducting, D-shaped device scheduled for construction at the ENEA Research Center in Frascati, Italy— will continue and expand upon this line of research. In its reference scenario, DTT allocates 6 MW of ICRF power (with a possible upgrade to 9 MW), contributing to a planned total heating budget of 45 MW. On DTT, the ICRF system is intended primarily for bulk-ion heating, reliable access to H-mode, and routine wall conditioning.

The present work therefore aims to systematically study DTT's ICRF heating capabilities and to explore novel operating configurations and heating schemes that could maximize overall device performance.

The paper is structured as follows: section 2 outlines the modelling strategy employed, detailing the use of full-wave codes to simulate the relevant physical processes and in section 3 profiles and simulation parameters of DTT are presented. In section 4 the analysis is presented and the results of the parametric sweep of the considered scenarios are discussed, finally section 5 draws the main conclusions and outlines directions for future work.

2 Modelling Strategy: 1-D and Full-Wave Solvers

Among the various techniques used to heat plasma, ICRF heating stands out for its use of radio frequency (RF) antennas—usually multi-strap designs—placed on the low-field side (LFS) edge of the plasma to launch fast magnetosonic waves. These waves travel through the plasma and transfer energy to both electrons and ions. Electron heating occurs via mechanisms such as Landau damping and transit-time magnetic pumping, while ion heating becomes significant when the wave frequency matches either the fundamental ion cyclotron frequency ($\omega = \omega_{ci}$) or its higher harmonics ($\omega = n\omega_{ci}$, $n \geq 2$). The propagation and absorption of these waves in a magnetized plasma are governed by a rich theoretical framework, as extensively developed in [2, 3].

While the theoretical principles governing the behavior of the waves are well established, their practical application in modern tokamak experiments involves a level of complexity that goes beyond analytical treatment. Factors such as realistic geometry, spatially varying plasma parameters, and intricate boundary conditions require the use of advanced computational modeling tools capable of accurately simulating the physical processes involved. In this context, a variety of numerical solvers have been de-

*Corresponding author: claudia.salvia@phd.unipd.it

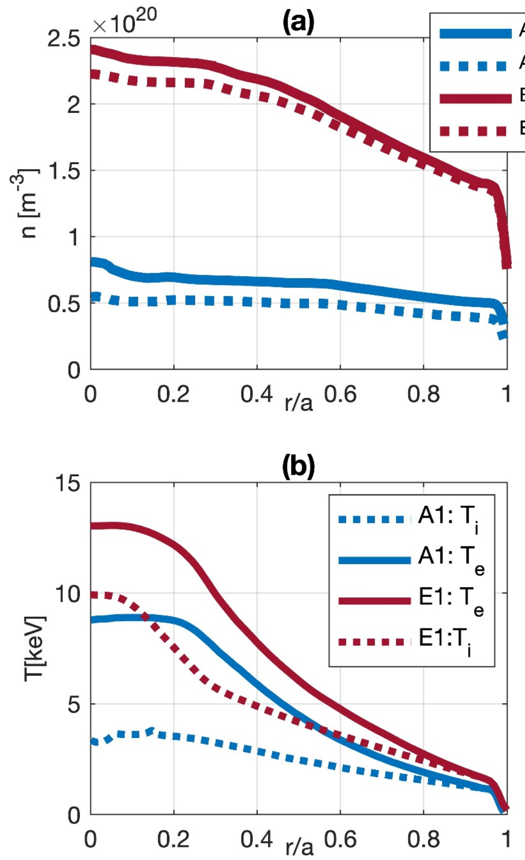

Figure 1. (a) Electron density profile n_e(r/a) and ion density profile n_i(r/a). (b) Electron temperature profile T_e(r/a) and ion temperature profile T_i(r/a).

veloped to address different aspects of ICRF wave behavior:

- One-dimensional (1D) kinetic full-wave solvers, such as TOMCAT [4] and FELICE [5], are capable of self-consistently modeling wave propagation and absorption along a single spatial coordinate, capturing key kinetic effects relevant to ICRF physics.
- More sophisticated multidimensional Maxwell–Vlasov full-wave codes—such as PION [6], LION, TORIC, CYRANO, EVE, and AORSA [7]—resolve the two- or three-dimensional geometry of the tokamak, incorporating realistic boundary conditions by modeling the metallic vessel wall as a perfect conductor, thus allowing a detailed simulation of wave behavior in the complex geometry of the device.

Because the wall forms an electromagnetic Faraday cage, multidimensional codes guarantee global power conservation: every watt of launched RF energy is absorbed somewhere inside the computational domain. Although this boundary condition is physically rigorous, it masks the intrinsic single-pass absorption efficiency of a heating scheme—a metric of paramount importance for scenario optimization. One-dimensional models, by contrast, compute local damping rates without the confining wall and

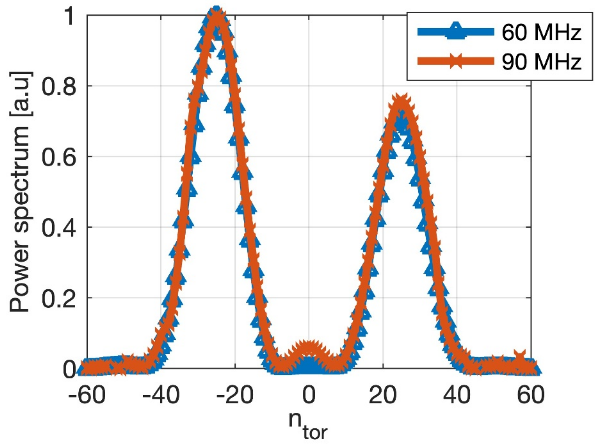

Figure 2. Antenna spectrum as function of toroidal mode number n_{tor}, at 60 MHz and 90 MHz.

therefore provide an unambiguous measure of the fraction of power absorbed during the first transit.

In the present work we exploit the complementary strengths of both approaches: TOMCAT is used to perform an extensive parametric survey of single-pass absorption, while TORIC and EVE validate the most promising cases in the full DTT geometry and deliver the detailed two-dimensional wave-field structure. This dual-model strategy yields a rigorous and comprehensive assessment of ICRF heating performance.

3 Plasma Profiles and Computational Settings

Building on earlier investigations [8, 9], this study explores the parameter space with three primary objectives: (i) to corroborate the full-field heating scenarios previously adopted for DTT, (ii) to re-examine three-ion configurations that had previously been observed, but not yet analyzed in terms of single absorption or subjected to a frequency scan, and (iii) to identify efficient ICRF options for the machine's initial, reduced-field campaign.

Numerical analyses were therefore performed at two toroidal-fields, 3 T and 6 T, corresponding to the successive operational stages of DTT. The 3 T configuration (scenario A1) represents the reduced-field commissioning phase, whereas the 6 T configuration (scenario E1) is the full-field reference case. It should be noted that in this paper the notation D(H) refers to minority heating schemes, while the notation D–H is used for schemes based on first harmonic heating (n=2), where no clear minority species can be identified. At 6 T we revisited the standard minority schemes—D(H) and D(^{3}He)—and re-examined an advanced three-ion mixture, (^{3}He)-D–H, building on the findings of [10]. For the 3 T configuration we analysed D-H and D-^{3}He, which remain the most promising avenues for reliable H-mode access at lower field. The electron-density, electron-temperature, and ion-temperature profiles employed in all simulations are derived from the latest

DTT transport projections (Fig. 1) and are summarised in Table 1.

Table 1. Main parameters of DTT heating scenarios

Parameter	A1	E1
Major radius R_0 [m]	2.19	2.19
Minor radius a [m]	0.7	0.7
Toroidal field B_0 [T]	2.92	5.84
Plasma current I_p [MA]	2.2	5.5
Central electron temperature T_{0e} [keV]	8.78	13
Central ion temperature T_{0i} [keV]	3.34	9.9
Central electron density n_{0e} [m^{-3}]	8.10×10^{19}	2.41×10^{20}

Boundary conditions were imposed through the three-strap ICRF antenna foreseen for DTT [11], which operates between 60 and 90 MHz, the power spectrum of which is shown in Fig. 2. The peak toroidal mode number, $n_{tor} = k_{\parallel} * R_0 = 25$, was adopted as the reference for the analyses in all codes, ensuring a uniform launch condition throughout. For further studies related to n_{tor}, see [12].

4 Analysis and results

The following sections present the main results of the studies for both reduced and full field scenarios, with a focus on the impact of ion composition and frequency.

4.1 A1: Reduced Field Scenario

To better understand the heating scenario in reduced magnetic field configuration, it is essential to analyze the accessibility of cyclotron resonance layers for different ion species. Figure 3 shows the positions of the cyclotron resonances for D, H, and ^{3}He as a function of RF frequency in the 3T configuration. The figure includes the resonance locations for the main isotopes up to the second harmonic (n=3). It is evident that on the high-field side, no fundamental resonance layer for H (purple curve) or ^{3}He (yellow curve) lies within the frequency range accessible by the DTT antenna. Instead, the presence of higher harmonics becomes significant: both the first harmonic (n=2) of ^{3}He (green dotted curve) and the first harmonic of H (blue curve) enter the accessible plasma region, potentially enabling effective heating at these locations.

Based on the plasma profiles defined in section 3, dedicated analyses were carried out using TOMCAT by varying the concentrations of H and ³He in a deuterium majority plasma as a function of frequency.

Figure 4 presents the single-pass absorption of H in deuterium plasma as a function of both H concentration and RF frequency. Two distinct absorption regions are visible: a prominent peak at higher frequencies, corresponding to the first harmonic of hydrogen, and a noticeable contribution at lower frequencies, associated with the fundamental resonance. The plot clearly shows that the single-pass absorption by H increases with the H concentration, reaching values above 70% in the optimal parameter range (approximately 78% on H and 10% on electrons).

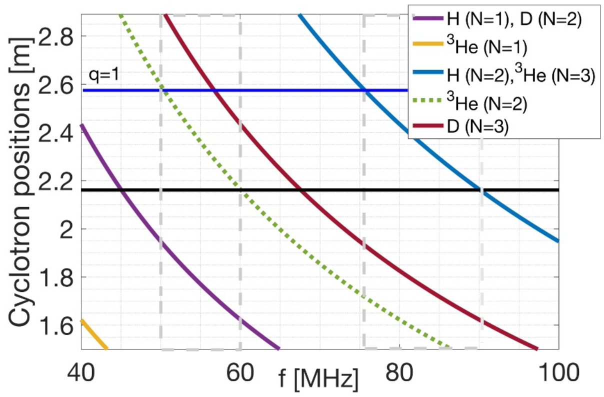

Figure 3. Location of the ion cyclotron resonance layers at $B_0 = 2.92$ T as a function of RF frequency. The black line indicates the position of the DTT magnetic axis, while the blue line corresponds to q = 1 safety factor surface.

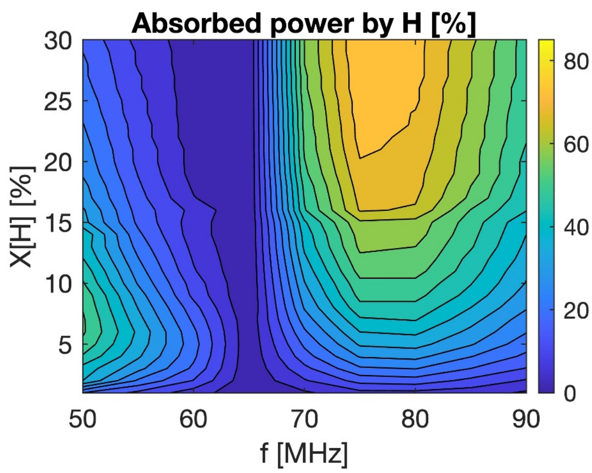

Figure 4. Single pass absorption of H minority in D plasma as function of the H concentration and frequency, as computed by TOMCAT for $n_{tor} = 25$.

The observed trend was further investigated using EVE, as shown in Fig. 5, with particular attention to the frequencies corresponding to the first-harmonic peak (80, 85, and 90 MHz), which consistently confirm the same behavior. In particular, it shows the power repartition between ions and electrons as a function of H concentration. A growing fraction of power is transferred to the ions as the H concentration increases up to about 40%. Beyond this value, the ion trend exhibits a slight but negligible reduction, rather than reaching a true flat-top, indicating only a weak saturation effect at higher concentrations. The trend reflects a transition from electron Landau damping at low H concentration to dominant ion cyclotron damping at higher concentrations, with weak saturation beyond 40% H. This consistency between TOMCAT and EVE provides robust validation for the identified heating regimes. Moreover, these results were further supported by additional simulations performed with TORIC code, which showed a consistent trend as a function of H concentration.

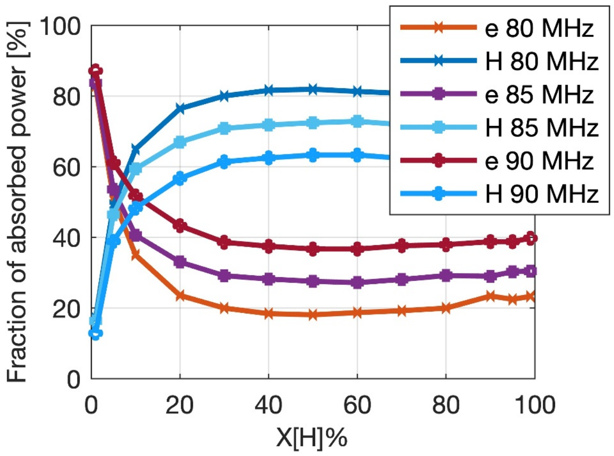

Figure 5. Partition of absorbed power by H ions and electrons as a function of H concentration for different RF frequencies (80, 85, and 90 MHz), as calculated by EVE for n_{tor} = 25.

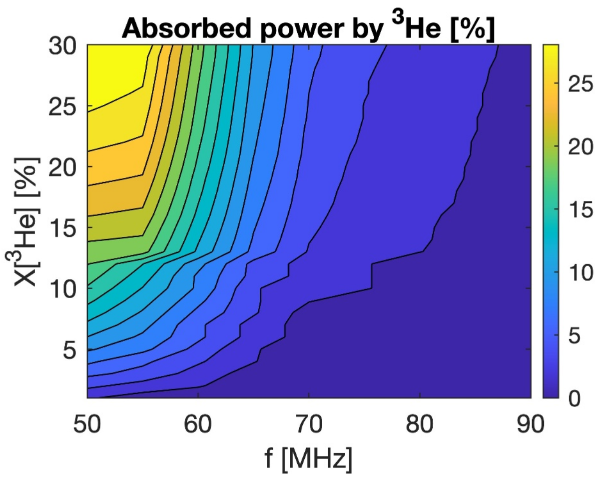

Figure 6. Single pass absorption of ^{3}He minority in D plasma as a function of the ^{3}He concentration and frequency, as computed by TOMCAT for n_{tor} = 25.

A similar analysis was performed for the D-^{3}He case. As shown in Fig. 6, a peak in absorption appears in correspondence with the first harmonic region, which is located just below the operational frequency range of DTT. In this scenario, an absorbed power fraction of about 30% is achieved when $X[^3\mathrm{He}] \approx 30\%$. The EVE simulations (Fig. 7), performed at 60 MHz within the operational limits of the DTT antenna, exhibited a similar trend to the D-H case, but with the flat-top behavior occurring at approximately 30% ^{3}He concentration. This behavior reflects the progressive shift from electron Landau damping to dominant ^{3}He ion cyclotron damping, while deuterium absorption remains negligible.

It should also be noted that, alongside its lower maximum absorbed power by the ion species (with a total first pass absorption of 30% on ^{3}He and 22% on electrons), the D-^{3}He configuration is less practical due to the higher procurement costs associated with helium relative to hydrogen. Moreover, past experimental campaigns conducted at JET have demonstrated very satisfactory results with H majority configuration, highlighting its effectiveness under realistic plasma conditions [13]. Therefore, these results support the selection of the D-H configuration as the most favorable option for the initial operational stages of DTT.

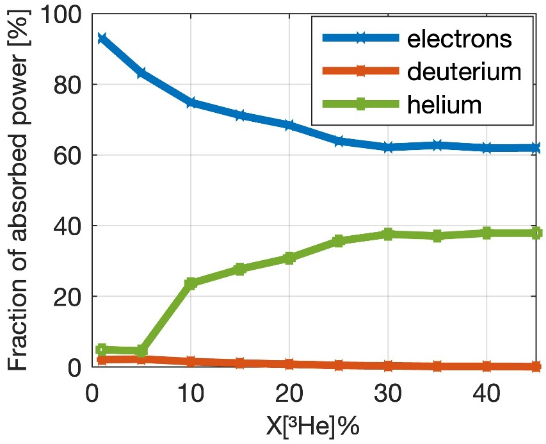

Figure 7. Partition of absorbed power by ^3He ions and electrons as a function of ^3He concentration, as calculated by EVE for n_{tor} = 25 and f= 60 MHz.

4.2 E1: Full Field Scenario

In the full field scenario, the heating strategy relies on conventional minority heating at the fundamental harmonic (n = 1). In this regime, the relevant resonance layers are the ³He fundamental, located in the 50–60 MHz range, and the H fundamental, present in the 75–90 MHz range. Figure 8 shows the position of these cyclotron resonance layers as a function of RF frequency, indicating the accessible regions for efficient power deposition. Accordingly, single-pass absorption analyses were conducted by TOMCAT (Fig. 9). For the D(H) case, two distinct absorption peaks are identified between 70 and 75 MHz. Despite providing optimal absorption for the minority, these frequencies yield predominantly off-axis heating profiles (see Fig. 10). Therefore, an operational scenario within the 85–90 MHz range is preferable: although the absorption is reduced by approximately 10–20%, the resulting heating is centrally localized (Fig. 10), which is more advantageous for plasma performance. For instance, at 85 MHz, the single-pass absorption reaches 52% on H, 17% on D, and 29% on electrons.

The minority heating D(^{3}He) scenario likewise displays an absorption peak close to 60 MHz, with about 50% of the power absorbed by the minority species and 37% by electrons (see Fig. 9).

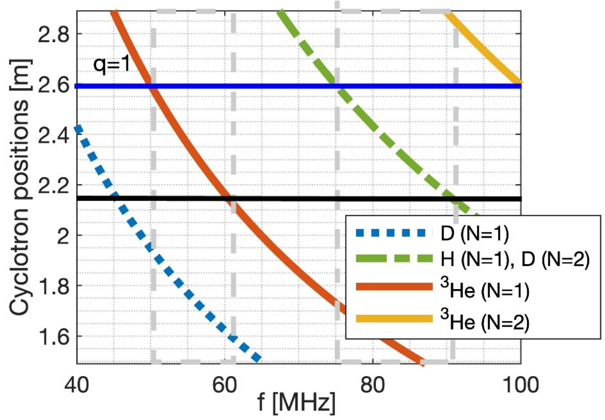

Figure 8. Location of the ion cyclotron resonance layers at $B_0 = 5.84$ T as a function of RF frequency. The black line indicates the position of the DTT magnetic axis, while the blue line corresponds to q = 1 safety factor surface.

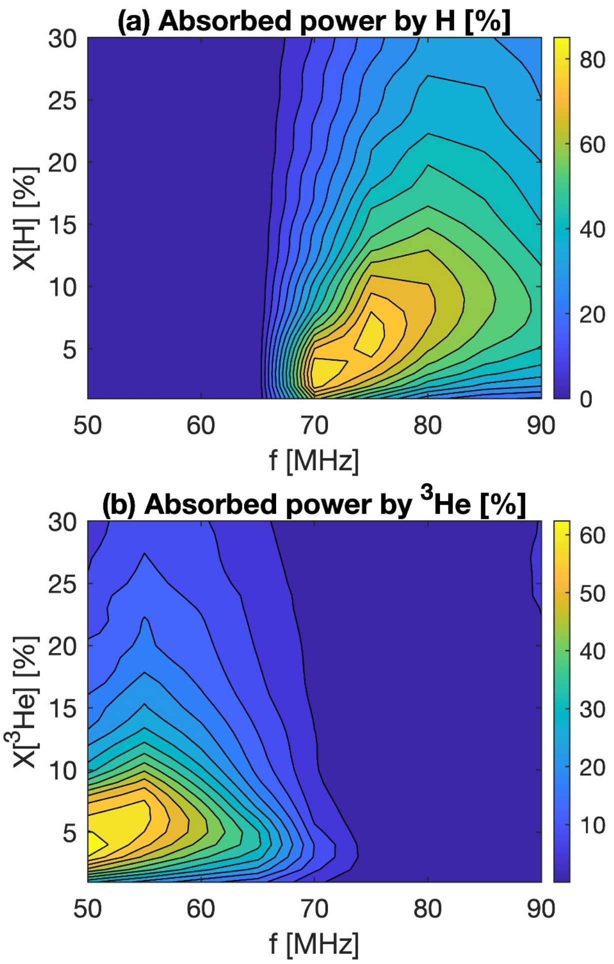

Figure 9. Single-pass absorption for D(H) (a) and D(^{3}He) (b) as a function of ion concentration and RF frequency, as computed by TOMCAT for $n_{tor} = 25$.

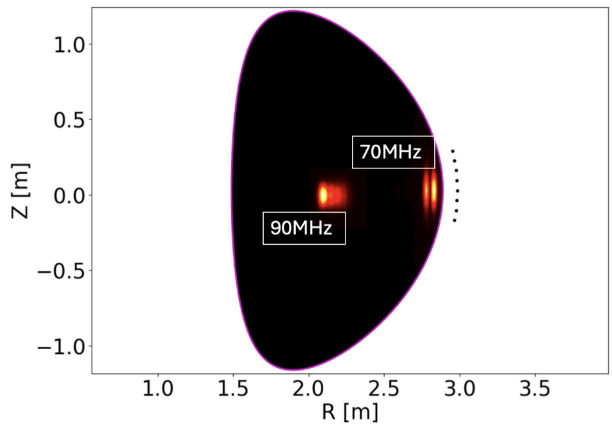

Figure 10. Poloidal cross-sections of the plasma illustrating the position of the power deposition peak for a D(H) plasma composition with 5% H, at 70 MHz and 90 MHz.

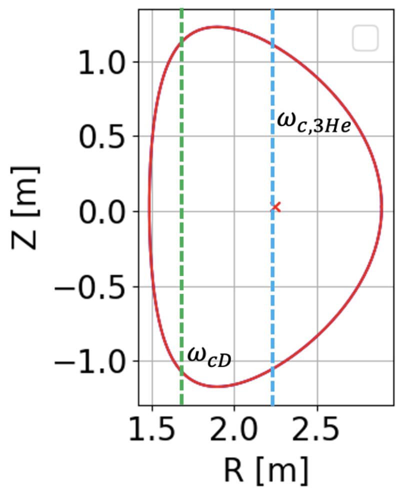

Figure 11. Poloidal cross-sections of the plasma at f=60 MHz showing D (green) and ^{3}He (blue) cyclotron resonance layers. The red cross marks the position of the power deposition peak for X[H]=71% and X[^{3}He]=0.02%.

The three-ion (^{3}He)-D–H configuration was also evaluated for the full field scenario, as illustrated in Fig.11, where the D and ^{3}He cyclotron resonance layers are shown. Three distinct regions of maximum power absorption are identified (see Fig.12); however, in the latter two, electron absorption is predominant, making only the first region particularly relevant for efficient ion heating. In this first region, single-pass absorption on the ^{3}He fundamental resonance reaches approximately 75% on ^{3}He (and 24% on electrons), as further confirmed by TORIC and EVE simulations (see Fig. 13, for f = 60 MHz). These results indicate that the three-ion scheme is a highly promising candidate among the full field heating configurations, offering even higher absorption fractions than the traditional two-ion scenarios. Nevertheless, as is well known, the practical implementation of this scheme is more challenging due to the need for precise control of low minority ion concentrations. A more detailed investigation of addi-

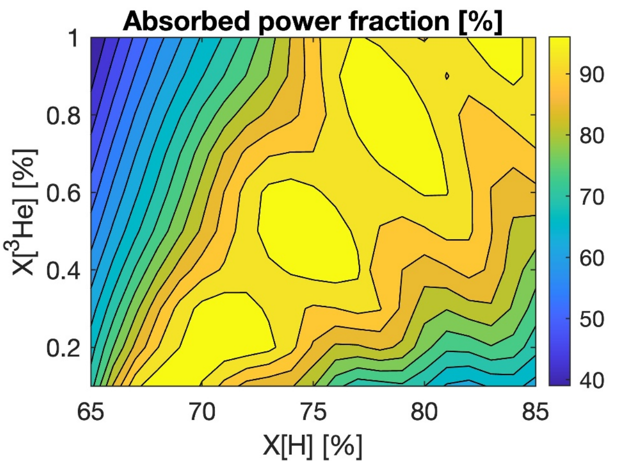

Figure 12. Single-pass absorption for the three-ion scheme (^{3}He)-D–H at f=60MHz, shown as a function of ^{3}He and H concentrations, as computed by TOMCAT for n_{tor} = 25.

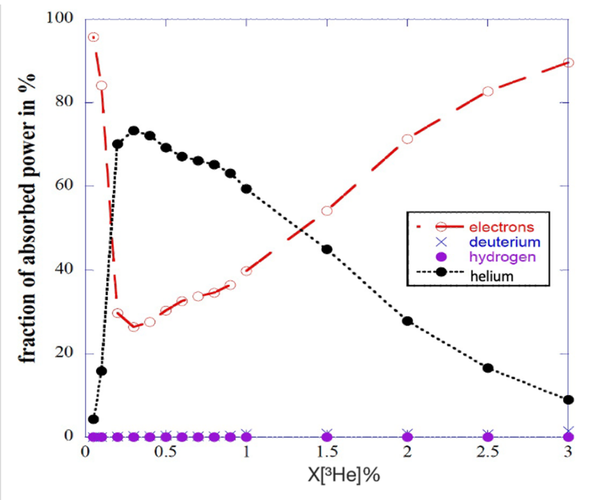

Figure 13. Partition of absorbed power by each species as a function of ^{3}He concentration at at f=60MHz, as computed by TORIC, in the three-ion scheme.

tional favourable three-ion scenarios for DTT is planned for future work.

5 Conclusions and future prospective

This study presents a comprehensive simulation-based analysis of ICRF heating scenarios for both reduced-field (A1) and full-field (E1) configurations in the Divertor Tokamak Test facility. The investigation employs the one-dimensional full-wave code TOMCAT, with additional validation provided by the TORIC and EVE codes. The modelling systematically explores a wide range of plasma compositions and RF frequencies, providing valuable insights for the optimization of ion heating performance in DTT.

The principal findings from the numerical analysis are summarised as follows:

- Reduced-field scenario (A1): the simulations indicate that the most favourable ion heating scheme is D-H heating at very high hydrogen concentrations $X[H] \geq 40\%$, where the absorption peak is maximised in the frequency range of 85–90 MHz. This configuration stands out for its efficient power deposition and heating effectiveness.
- Full-field scenario (E1): the effectiveness of minority heating schemes is reconfirmed, in agreement with previous analyses [8, 9]. As a novel contribution, this study proposes a three-ion heating scenario characterized by X[H] = 71%, X[^{3}He] = 0.2%, and a frequency of 60 MHz, which proves to be highly effective in terms of single-pass absorption. Future work will address other three-ion configurations potentially favourable for DTT.

These findings offer valuable input for future optimisation of the DTT ICRF system, with the reduced-field D-H first harmonic (n=2) heating scenario emerging as a particularly promising candidate for further experimental study.

6 Acknowledgment

One of the authors (AC) acknowledges support by Italian National Group for Mathematical Physics of Istituto Nazionale di Alta Matematica (INdAM).

The PhD in the framework of which the activity has been performed is co-funded by Eni S.p.A. within the Piano Nazionale di Ripresa e Resilienza (PNRR) of the Italian Government.

This research has been carried out within the framework of the EUROfusion Consortium, funded by the European Union through the Euratom Research and Training Program (Grant Agreement No. 101052200 - EUROfusion). Additionally, this work is funded by the European Union, NextGenerationEU. Views and opinions expressed are, however, those of the author(s) only and do not necessarily reflect those of the European Union or the European Commission. Neither the European Union nor the European Commission can be held responsible for them.

References

[1] F. Romanelli et al., Divertor Tokamak Test facility Project: Status of Design and Implementation. Nucl. Fusion **64**, 112015 (2024). https://doi.org/10.1088/1741-4326/ad5740

[2] T.H. Stix, Waves in plasmas, (Springer Science & Business Media, 1992)

[3] M. Brambilla, Kinetic theory of plasma waves: homogeneous plasmas, (Oxford University Press, 1998)

[4] D. Van Eester et al., A variational principle for studying fast-wave mode conversion. Plasma Phys. Control. Fusion **40**, 1949 (1998). https://doi.org/10.1088/0741-3335/40/11/010

[5] M. Brambilla, Finite Larmor radius wave equations in Tokamak plasmas in the ion cyclotron frequency range. Plasma Phys. Control. Fusion **31**, 723 (1989). https://doi.org/10.1088/0741-3335/31/5/004

[6] L.G. Eriksson et al., A model for calculating ICRH power deposition and velocity distribution. Physica Scripta **52**, 70 (1995). https://dx.doi.org/10.1088/0031-8949/52/1/014
[7] R. Bilato et al., Status of the benchmark activity of ICRF full-wave codes within EUROfusion WPCD and beyond, AIP Conf. Proc. **1689**, 060001 (2015). https://doi.org/10.1063/1.4936499
[8] A. Cardinali et al., Study of ion cyclotron heating scenarios and fast particles generation in the divertor tokamak test facility. Plasma Phys. Control. Fusion **62**, 044001 (2020). https://dx.doi.org/10.1088/1361-6587/ab73da
[9] A. Cardinali et al., Numerical Investigation of the Ion Cyclotron Resonance Heating (ICRH) Physics in DTT. Journal of Physics: Conference Series **2397**, 012017 (2022). https://dx.doi.org/10.1088/1742-6596/2397/1/012017
[10] Y.O. Kazakov et al., On resonant ICRF absorption in three-ion component plasmas: a new promising tool for fast ion generation. Nucl. Fusion **55**, 032001 (2015). https://dx.doi.org/10.1088/0029-5515/55/3/032001
[11] S. Ceccuzzi et al., Progress in the development of the ICRF system of DTT. Fusion Engineering and Design **213**, 114849 (2025). https://doi.org/10.1016/j.fusengdes.2025.114849
[12] A. Cardinali et al., ICRH modelling of DTT in full power and reduced-field plasma scenarios using full wave codes. Plasma Phys. Control. Fusion **67**, 085018 (2025). https://doi.org/10.1088/1361-6587/adf774
[13] E.A. Lerche et al., N= 2 ICRH of H majority plasmas in JET-ILW. AIP Conf. Proc. **1689**, 040003 (2015). https://doi.org/10.1063/1.4936486